applied mechanics

MDPI

Article

Experimental Study of the Stress State of a Polymer Composite in a State of Compression

Anatoliy Ishchenko [1], Volodymyr Kravchenko [1], Artem Arustamian [2,*], Dmytro Rassokhin [3], Dimitrij Seibert [3], Olena Nosovska [1], Robert Böhm [3] and Stanislav Kapustin [1]

[1] Department of Mechanical Equipment, Pryazovskyi State Technical University (PSTU), 49005 Dnipro, Ukraine; ischenko50@ukr.net (A.I.); kvm1249@gmail.com (V.K.); nosovska_o_v@pstu.edu (O.N.); stanislav.kapustin.engineer@gmail.com (S.K.)
[2] Department of Foundry Engineering, AGH University of Krakow, 30-059 Kraków, Poland
[3] Faculty of Engineering, Leipzig University of Applied Sciences, 04277 Leipzig, Germany; dmytro.rassokhin@htwk-leipzig.de (D.R.); dimitrij.seibert@htwk-leipzig.de (D.S.); robert.boehm.1@htwk-leipzig.de (R.B.)
* Correspondence: aac0979560476aac@gmail.com

Abstract: Long-term operation of the supporting surfaces of large-sized parts, in particular tubular units of thermal power plants, leads to the destruction of the contact surfaces. Moisture penetrates into the formed discontinuities, and the vibrations present in the equipment in use rapidly increase the gap, reaching values of 10–15 mm. The authors of this article proposed the application of a composite layer of multimetal 1018 material without performing additional preparatory operations, ensuring the mandatory penetration of the material into the body of the supporting surface. This depth provides additional stability by maintaining boundary conditions. To determine the rational thickness of the composite layer, mathematical modeling of static loading of samples with different thicknesses in a wide range of values (from 2 mm to 12 mm) was performed. It was determined that the effective implementation of the developed technology was possible due to an increase in the load-bearing capacity of the composite material by creating additional grooves, or artificially creating grooves by welding, in the body of the part with a depth of 2.5–3 mm. The optimal excess of the composite was 1.0–1.5 mm. The proposed technology increases the stability of the composite layer up to three times and allows restoration without the use of mechanical treatment. The increase in the maximum stress values was 770 MPa, compared to the standard technology of 205 MPa.

Keywords: composite material; restoration; supporting surfaces; thermal power plants; strength

Citation: Ishchenko, A.; Kravchenko, V.; Arustamian, A.; Rassokhin, D.; Seibert, D.; Nosovska, O.; Böhm, R.; Kapustin, S. Experimental Study of the Stress State of a Polymer Composite in a State of Compression. *Appl. Mech.* **2024**, *5*, 619–633. https://doi.org/10.3390/applmech5030035

Received: 22 April 2024
Revised: 9 August 2024
Accepted: 1 September 2024
Published: 10 September 2024

1. Introduction

In the Pryazovskyi State Technical University, new technologies for power equipment repairs have been developed by using modern composite materials. The widespread use of composite materials in various industries, primarily when performing repair or installation work, necessitates a deeper study of both the properties of various materials and the features of their use under static and dynamic loads. A significant number of works devoted to the use of composites do not provide an answer to a number of questions regarding the optimal values of the use of a layer of composite material that can withstand a compressive load and the resulting ultimate stresses [1–5]. Research on the rehabilitation of rolling equipment with composite materials is noteworthy [6]. However, the issues of calculation of stresses arising in the process of operation were not studied in that research.

The restoration of foundation slabs is a complex technological process, including the provision of a tight fit and high surface finish [7].

The technology for installing foundation plates for turbines, Leningrad Metallurgical Plant and Ural Turbomotor Plant (type LMZ and UTMZ), includes the installation of embedded steel plates, followed by concreting in the upper cord of the foundation. At the

same time, permanent linings are installed between the embedded plate and the foundation frame of the turbine unit. Both contact surfaces of the permanent pad are scraped to ensure maximum contact. Such mounting of the plate ensures the durability of the structure even in the presence of vibrations.

However, during operation, high temperature, humidity, and the presence of stray currents in the operated units lead to the development of corrosion [8]. Such wear contributes to an increase in the gap in the adjacent surfaces and, as a result, to an increase in the magnitude of vibration [9]. Restoration of the broken contact is provided by replacing the permanent lining, with further alignment of the foundation and fitting operations. It should be noted that this process requires highly qualified personnel, as well as equipment that allows scraping surfaces with high cleanliness. In this regard, it became necessary to develop a repair technology that can significantly simplify the entire process, as well as reduce costs.

Researchers have developed and successfully applied technology for repairing cracks using a self-healing composite [7].

Such composite consists of an epoxy matrix and contains encapsulated dicyclopentadiene (DCPD) and a first-generation Grubbs Ru-catalyst. The use of this repair technology made it possible to increase the fatigue life to 118%, and with moderate destruction, it extended the fatigue life to 213% [10].

However, the disadvantages of this technology include the high cost of producing encapsulated epoxy composites [11]. In addition, they have low mechanical properties, which greatly limits their scope of application and precludes their use in large structures [12].

The use of self-healing technology based on polyurethane modified with carbon nanotubes, as well as carbon fibers is well known [13]. The study involved repairing a cut-type lesion. In this case, recovery was ensured by heating the damaged samples to 60 °C for 30 min. The recovery was up to 72% of the original strength. This repair technology is difficult to implement for large parts of metallurgical production.

To increase the elasticity of polymers, plasticizers are introduced into their composition [14]. To increase resistance to heat and light and prevent changes in the properties of compounds during operation, special stabilizers are added [15]. A number of other components added to repair compositions, such as thickeners, accelerators, thixotropic additives, modify the compound of the composition, improving mechanical, technological or operational characteristics [16]. The result of such improvements has been a surge in activity in the use of new polymer compositions in various types of repairs, including the restoration of machine parts operating in heavy industry. A whole group of companies developing such materials has appeared on the world market. These include a group of German companies (MultiMetall Reiner Schulze e.K., Viersen, Germany and DIAMANT Polymer GmbH, Mönchengladbach, Germany), a group of American companies (Loctite Westlake, OH, USA, Devcon North America, Danvers, MA, USA, A.W. Chesterton Company, Groveland, MA, USA and Belzona, Inc., Miami, FL, USA, The Thortex Group, Collegeville, PA, USA), as well as DURMETAL AG (St. Niklausen (OW), Kerns, Switzerland) and Chester Molecular Ltd. (Łomianki, Poland).

A distinctive feature of repair polymer compositions from the glue connections on the basis of which they are created is the ability of these compositions to perform specified functions at sufficiently large thicknesses of the applied material. If glue connections are characterized by a thin film of applied glue (0.01–0.10 mm), then when using metal-polymer compositions, the layer of applied material can be from 0.5 mm to 10 mm or more [17]. That is, repair polymer compositions are actually form-building materials with which a wide range of repair problems can be solved, such as restoration of working surfaces, building up and adjusting.

The use of these materials seems to be most effective in those industries where, for one reason or another, it is impossible to use traditional repair technologies, including welding. Such reasons include fire safety requirements, the impossibility of a long-term shutdown of production, adverse thermal effects on the part being restored and the need to use special technologies (for example, welding cast iron parts) [18].

Employees of Pryazovskyi State Technical University have developed a technology for restoring supporting surfaces using material from the German company DIAMANT Polymer GmbH Mönchengladbach, Germany. And also, a complex study of the properties of composite materials was carried out: in particular, the composite material multimetal 1018 of this company. At the same time, the authors of the technology made an assumption about applying a polymer material into technological grooves made on the supporting surface. This should increase the bearing capacity of the polymer layer under compression [17]. At the same time, the question of the optimal values of the magnitude of such a deepening, as well as the question of determining the ultimate loads perceived by such a design of the polymer carrier layer, remains absolutely not clarified. The study of this issue by direct experimental means requires not only considerable time, but also a multifactorial experiment, taking into account at least three factors, in particular, the thickness of the layer, consisting of sections with and without deepening and the geometric parameters of deepening. Such a task is quite complex and time-consuming when performed in laboratory conditions. In this regard, a study of the named problem was carried out using computer simulation and the optimal values of the mentioned parameters were established. To assess the elastic properties of composite materials, researchers quite effectively use the finite element method [19–21]. The final results were tested in laboratory conditions, with further application at an operating enterprise. This article is devoted to the development of the proposed technology and its testing.

The purpose of this study is to determine the optimal values for the deepening of the composite material multimetal 1018 into the body of the restored part and the thickness of the composite layer of the material, which exceeds the zero level of the part. The task of this study is to develop a technology for the restoration of supporting surfaces, taking into account the results of computer modeling and laboratory studies of the stability of the composite layer.

2. Materials and Methods

Multimetal Steel 1018 is a two-component metal polymer based on specially selected epoxy resins and stainless (corrosion-resistant) metal fillers. Its area of application is the use during installation or replacement of bridge supports to level the supporting surfaces or seal gaps of various sizes that form between the bridge structure and the support. After hardening, it has high compressive strength and long-term chemical resistance.

Thanks to its perfectly balanced viscosity, it is easily applied to base plates and wedge gates and is evenly distributed during installation, thereby simultaneously filling gaps and installing supports in the final position. There is no need for machining, which is time-consuming and costly during normal fitting. Thanks to the release agent from Diamant ("Diamant" Trennmittel), it is possible to dismantle the supports sometime later.

To perform the tests, the composite material multimetal 1018 of the German company DIAMANT Polymer GmbH Mönchengladbach, Germany was selected. The technical specification is given below (Table 1).

Table 1. Technical characteristics of multimetal 1018.

Parameter	Unit	Value
Ultimate compressive strength	N/mm^2	max.160
Ultimate Tensile Strength	N/mm^2	76
Shear strength	N/mm^2	89
Ultimate strength in bending	N/mm^2	22
Modulus of elasticity	N/mm^2	14,000
Linear elongation coefficient		32×10^{-6} K
Temperature stability—long-term	°C	−40/+ 90 °C

Table 1. *Cont.*

Parameter	Unit	Value
Clutch friction coefficient		>0.5
Processing time at +20 °C	min.	~45
Hardening time at +5 °C	hour	~72
Hardening time at +20 °C	hour	~24
Specific gravity	g/cm^3	2.4

2.1. Preparation of the Samples

To determine the effectiveness of the developed technology, it was proposed to study the resistance of composite samples in various formats of its location on the supporting surface (Figure 1).

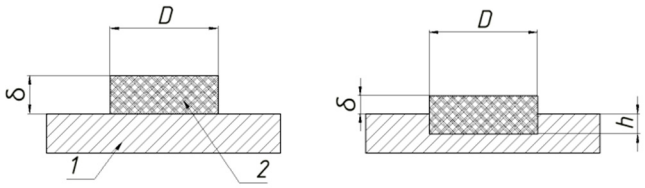

(**a**) (**b**)

Figure 1. Scheme of the test sample (**a**) in a free form and (**b**) in a fixed form. Steel sample 1 with a deposited composite layer 2 with a diameter *D*, a thickness of the recess in the metal body *h* and an excess of *δ*.

Both types of specimens were studied under compressive loading. The following characteristics of the samples were optimized: the depth of the composite sample in the body of the part h; excess of the sample over the surface of the part δ. The sample diameter D remained constant.

2.2. Simulation

The search for optimal parameters was carried out by the method of mathematical modeling in the Ansys system. This system was used to create the model, generate meshes, and perform finite element calculations. The modeling process begins with the creation of individual elements with a given geometry, followed by assembly into a complete integrated model. Objects were modeled using continuum elements. The properties of the polymer were taken from the technical characteristics of the material presented above. As a model for the deformation of the polymer sample, the elastic-ideally plastic model was chosen [22]. The structure analysis was carried out on the basis of the obtained results of the von Mises equivalent stress and the total strain.

A compressive load was applied to a flat cylindrical surface, while the object of parametrization was the characteristic *h* (sample penetration) and the excess *δ* (Figure 2).

In addition, during the simulation, contact stresses were determined according to the proposed scheme (Figure 3). Figure 3 shows the layout of the points along the model cross-section where contact stresses are measured. Points 1, 2, 3 and 4 were chosen to model the contact stress in the following locations: Point 1: at the contact boundary between the material and the side wall of the recess; Point 2: in the stress concentration zone; Point 3: in the area of material contact with the inner surface of the seating recess and Point 4: in the area of material contact with the pad surface. This stress measurement scheme makes it possible to evaluate the nature of the sample deformation over the entire cross section.

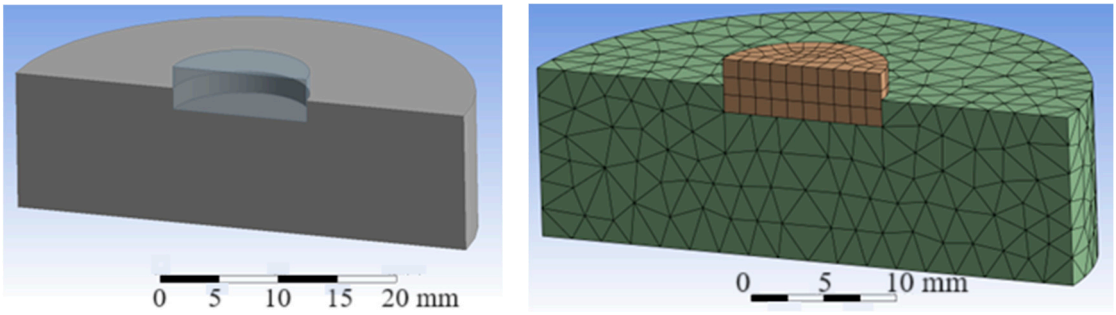

(**a**) (**b**)

Figure 2. 3D models of (**a**) the fixed specimen with the composite specimen installed and (**b**) with the finite element mesh applied.

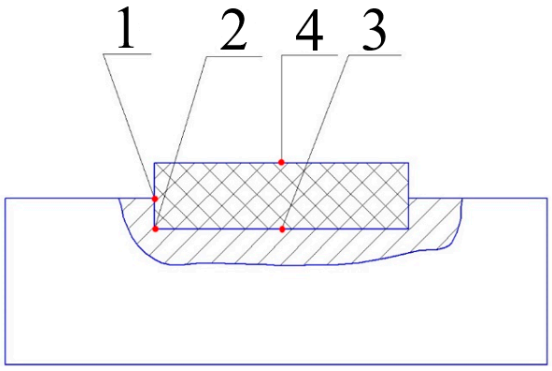

Figure 3. Scheme of location of points along the cross section of the model. Points on the diagram (1, 2, 3 and 4) on which the contact stress modeling is performed.

To perform calculations using the finite element method, the Static Analysis module with parameterization was used (Figure 4). Geometric values corresponding to the research task (excess, recess, diameter and load) were selected as the variable range of parameters.

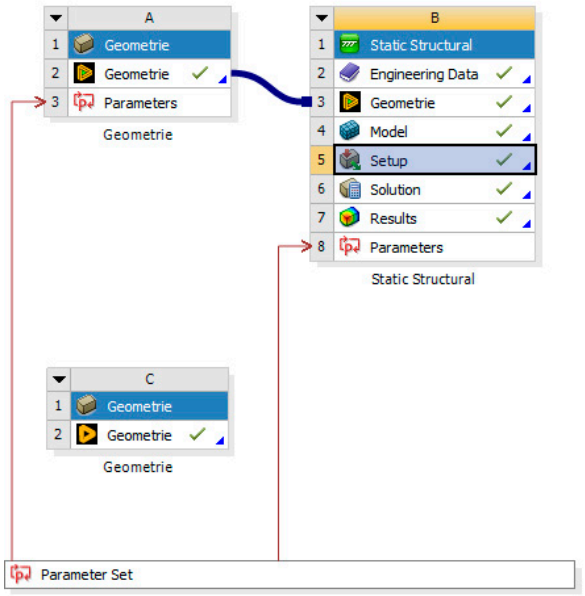

Figure 4. Calculation scheme in the module of "Ansys Workbench".

Loading simulation was performed using the "Force" type of load applied normal to the sample plane. To construct the finite element mesh, the Tet10 mesh type was used with a number of elements of 3238. The quality of the mesh is presented in Figure 5.

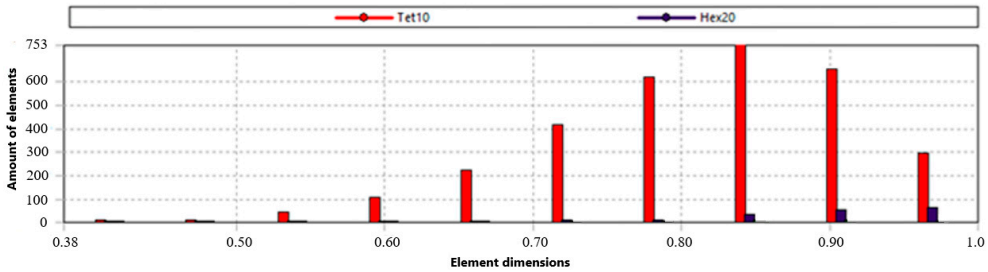

Figure 5. Finite element mesh quality.

2.3. Laboratory Experiments

Laboratory testing of the samples was carried out at room temperature, using the equipment of the State Higher Educational Institution "PSTU". The sample was subjected to static compression on a P-20 Universal Rupture Machine (RM20, Factory of testing machines ZIM TochMashPribor, Armavir, Russia) until destruction. The machine is designed for static testing of standard samples of metals, as well as polymers, for compression and tension. The load was recorded using an analogue dial. The greatest generated load is 200 kN.

Loading of the samples was carried out until the loss of resistance. The destruction of the sample was recorded in the form of a drop in the achieved force. In this way, the strength limits were obtained for each type of sample.

To conduct a laboratory experiment, the Young–Poisson model was used [23]. The main test method was compression [24]. The Young–Poisson model is an effective and frequently used tool for evaluating the elastic properties of materials. It is widely used in various fields of science and technology, providing high accuracy and reliability of results. This model is used by many authors in various studies, which is confirmed by numerous examples from the scientific literature [25–27].

The purpose of the experiment is to evaluate the resistance of the material under compressive loads. Equipment used in the experiment is a polymer sample, which is a flat disk placed in a cylindrical space, enclosed between two planes. At the same time, several options for installing a composite sample were considered. The first option is to freely install the sample on the surface. The second option is to install the sample in a recess that ensures tight contact along the side surface.

The number of test samples according to the experimental plan is 75 pieces, i.e., 15 pcs. for each diameter (D = 12 mm, D = 16 mm, D = 20 mm, D = 25 mm, D = 30 mm).

The conditional yield strength ($\sigma_{0.2}$) was calculated using the formula

$$\sigma_{0.2} = P_{0.2}/F_0 \quad (1)$$

where $P_{0.2}$ is the force applied to the specimen at which the conditional yield strength (0.2% strain) is reached and F_0 is the cross-sectional area of the specimen on which this force acts.

To determine the conditional yield strength, sequential loading and unloading of the test samples was performed. Loading was performed in several stages with a static load. The preload was no more than 10% of the expected load σ_0, providing the conditional yield stress. This preload was maintained for 10 s to stabilize the specimen before the main load. The specimen was then subjected to further loading until the desired strain level was reached and the yield strength was measured. At the next stage, the sample was loaded until the stress reached twice as high as the initial values $\sigma = 2\sigma_0$ and was maintained for 10–12 s, after which it was unloaded to the stress σ_0. Each time after the load was removed, the sample was measured in height and so was the amount of excess, which made it possible to determine the amount of shrinkage of the sample. The tests were stopped after the sample lost its shape, as well as at visible signs of destruction.

The experimental conditions during the experiment corresponded to an ambient temperature of 20 ± 2 °C, a loading speed of 10 kN/s.

As a result of loading the sample in various states, an increase in the durability of the composite was revealed. The reasons for the increase in resistance are based on several factors. When the sample is placed in a closed volume, boundary conditions are maintained. The added support reduces compression deformation and also creates a reinforced structure that provides additional rigidity and impact resistance. In addition, the closed volume ensured uniform load distribution throughout the entire volume of the sample. This prevented the formation of stress concentrations in certain areas and promoted more uniform compression. In addition, the closed volume ensured that the shape of the composite sample was retained under compression.

The strength of the composite under axial compression is determined by the formula [28]

$$\sigma_x = [E_a \cdot V_a + E_m \cdot (1 - V_a)] \cdot \varepsilon_a \quad (2)$$

where ε_a is the ultimate strain of fibers during compression.

As computer modeling has shown, the optimal depth values are h = 1.5 mm. It should be noted that the durability of the sample is also ensured by large-depth values up to 2–3 mm; however, it is not always possible to ensure such depth in the body of the part.

3. Results

Based on the analysis of the results, the dependence of the hardening of the core of the composite sample was found, due to the compaction of the material in a closed volume (Figure 6).

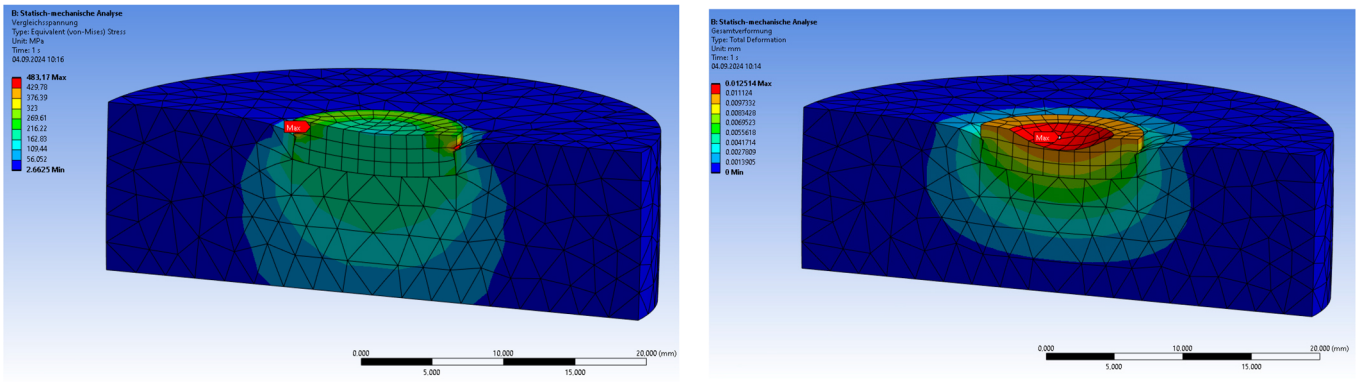

(**a**) (**b**)

Figure 6. Results of calculation (**a**) of stresses and (**b**) deformations obtained using the program "Ansys Workbench".

The next stage of studying the strength of multimetal under conditions of uniform compression is the consideration of the following characteristic points (Figure 3):

No. 1—at the contact boundary, the material is the side edge of the recess;
No. 2—in the stress concentrator;
No. 3—in the zone of contact of the material—inner surface of the fitting groove;
No. 4—in the zone of contact of the material with the pad of the rolling roll.

The Ansys Workbench application allows you to determine the percentage of the model volume in which stresses of a certain magnitude operate (Figure 7).

Thus, while processing the obtained data, it was found that the number of points on the diagram at which the stress value is maximum is insignificant (less than 1%); therefore for analysis, we accept those values of the maximum stresses in the contact zone of the sample, the base that correspond to 1% of the assembly volume and more. Stresses were analyzed within the same group of diameters, i.e., five samples each. The volumes of samples from one group differ little from another, so this factor can be neglected.

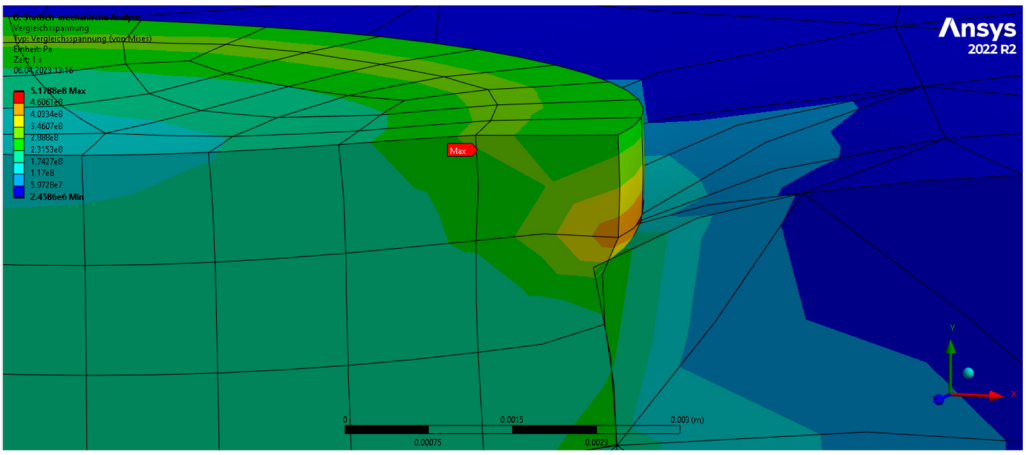

Figure 7. Stress distribution over the cross section of the sample.

With a value exceeding 1 mm at point No. 1, the stress value is 240 MPa; at point No. 2 and No. 3, about 120 MPa and No. 4, 82 MPa, i.e., twice less; and in the case of point No. 4, it was almost three times less in diameter sample by 20 mm. At the border of contact material—side edge (point No. 1), the stress value reaches 300 MPa, and at points No. 2–4, about 130 MPa at a value exceeding 1.5 mm, i.e., they differ by 2.3 times and for point No. 4, also by three times (98 MPa).

Stress at points No. 1, No. 2, No. 3 and No. 4 with diameter samples 12 mm and 16 mm are at the level from 28 to 100 MPa for all types of excess.

When increasing the diameter up to 25–30 mm, increase in stress at the points under study is observed when the diameter exceeds over 2 mm (about 320 MPa).

The obtained data of the dependence of polymer material exceedance on the stress value for all variants of specimen diameters were summarized in a single graph (Figure 8). The data for point 1 are presented here due to the fact that for other points, the material behavior was similar but with a smaller gradient.

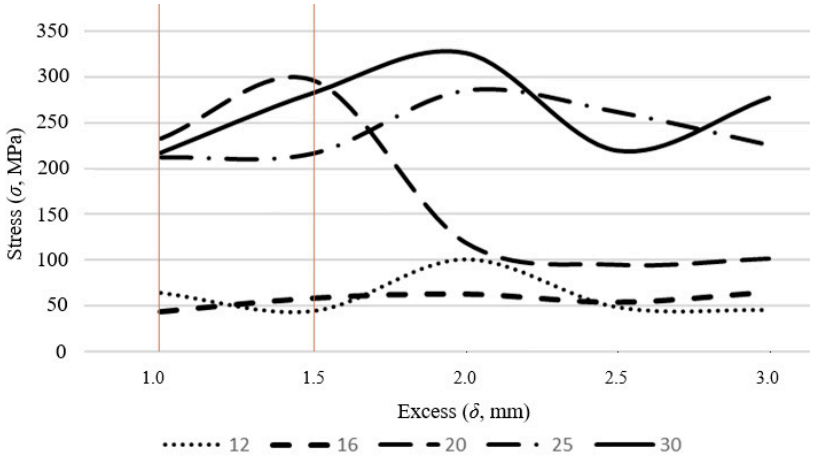

Figure 8. Graphical dependence of stress on excess value (for point 1, red lines highlight the region of highest stresses for all types of specimens).

The graph demonstrates how the stress in the polymer material changes with increasing exceedance values. Different specimen diameters (represented by values of 12, 16, 20, 25 and 30 mm) show different patterns of stress behavior. The highest stress increase for all types of specimens is observed in the region between 1.0 and 1.5 mm. Meanwhile, specimens 12 and 16 mm in diameter showed low load-bearing resistance, with similar stress levels throughout the entire exceedance range. What is evident is that as the con-

tact area increases, the bearing capacity of the metal-polymer material multimetal steel 1018 increases at the same normal force acting on the specimens.

Figure 9 shows a summary graph of the dependence of the polymer material burial on the stress value for all variants of specimen diameters.

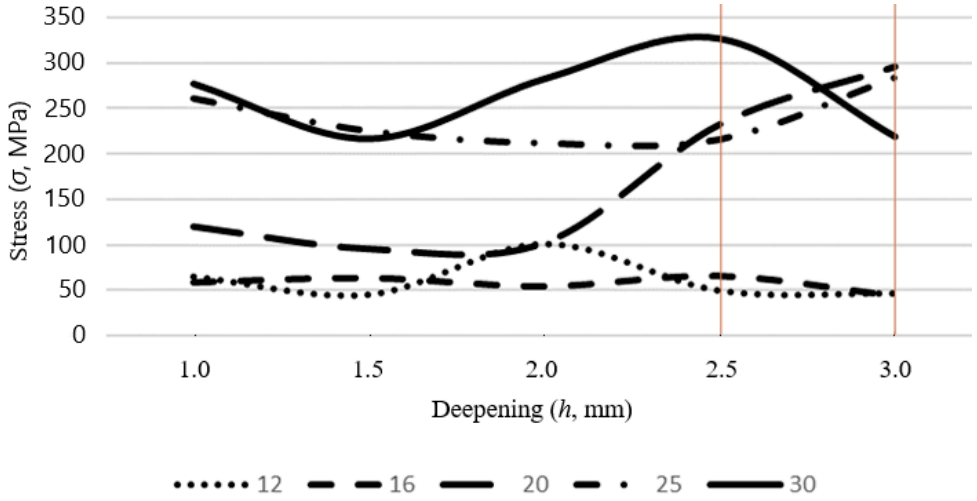

Figure 9. Graphical dependence of stress on the amount of material burial (for point 1, red lines highlight the region of highest stresses for all types of specimens).

It follows from the obtained data that the optimum value of burial is the range from 2.5 to 3.0 mm. At the same time, specimens with diameters of 12 and 16 mm behave similarly as in the study of the influence of the exceedance level.

The results of this study are consistent with the results of similar studies on composite materials in compression. For example, a study by the authors of [29] investigated the improvement of compressive strength in tin slag-based polymer concrete when confined by metal tubes. They reported a significant improvement in strength, with partial and full metal confinement resulting in 61.95% and 122.74% increase in strength, respectively, compared to unconfined specimens. This strength increase was attributed to metallic confinement altering the stress distribution and failure modes of the material, resulting in higher ductility and delayed fracture [29]. Forquin et al. [30] also studied the behavior of PMMA (polymethylmethacrylate) under confined compression, noting that confinement significantly affects the mechanical response of the material, increasing the compressive strength and altering the failure mechanisms. Strength gains for specimens confined in cylindrical rings were up to 40% at a maximum true strain value of 0.15. These comparisons confirm our results, highlighting the important role of metallic confinement in improving compressive strength and modifying the deformation behavior of polymeric materials.

To confirm the obtained calculations, we carried out experimental loading of a 30 mm-diameter specimen with the optimum values of exceedance and burial. At the same time, we were interested in the influence of a larger layer on the resistance of the polymer material in the range of values from 2 to 12 mm. In order to compare the obtained results, tests were also carried out for a free Figure 10 specimen.

Considering the maximum load (bearing capacity) for all diameters, we can identify the optimal value for exceeding, which ranges from 2.5 mm to 3.0 mm for the sample diameter of 30 mm. With these values, the maximum stresses are 770 MPa for a sample enclosed in a closed volume and 205 MPa for a freely fixed sample.

During laboratory studies, it was found that the load-bearing capacity of the composite layer increases significantly if part of the material is enclosed in a closed volume of a previously made recess on the supporting surface.

As can be seen in Figure 10, an excess of 2.5 mm in the material gives for a closed sample the critical stress values (at which the sample is destroyed) at the level of 770 MPa,

which corresponds to 205 MPa compared to the free version—an increase in resistance by more than three times.

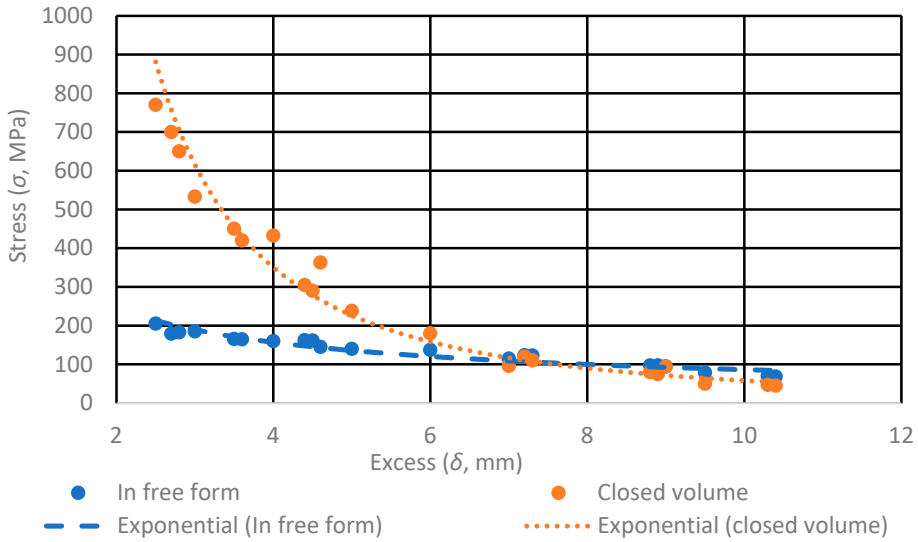

Figure 10. The dependence of the magnitude of the limiting stresses at various values of the excess of the composite layer of the sample for a free placement option and a sample located in a closed volume. Static loading. Results of laboratory tests.

In order to compare the accuracy of the results obtained by the simulation and laboratory test, Table 2 is shown.

Table 2. Data table of shrinkage values for samples of different diameters.

Group 1: Diameter Approx. 12 mm					
Sample No.	**Diameter (mm)**	**Load (kN)**	**Yield Strength $\sigma_{0.2}$ (MPa)**	**Real Shrinkage (mm)**	**Shrinkage Obtained by Modeling (mm)**
1	11.9	17.658	105.02	0.015	0.01531
2	11.8	14.715	91.54	0.010	0.01072
3	12.2	14.715	90.85	0.010	0.01328
4	11.9	11.772	70.40	0.010	0.01231
5	11.8	11.772	60.09	0.025	0.02772
Group 2: Diameter approx. 16 mm					
6	16.2	26.487	149.51	0.025	0.02233
7	15.9	23.544	129.12	0.015	0.02310
8	15.8	20.601	112.05	0.015	0.02233
9	15.9	20.601	93.59	0.030	0.02742
10	15.8	26.487	128.46	0.030	0.02310
Group 3: Diameter approx. 20 mm					
11	20.3	58.860	164.73	0.030	0.02691
12	20.0	58.860	142.85	0.030	0.03614
13	19.9	49.050	124.87	0.020	0.02749
14	20.1	68.670	162.22	0.035	0.03375
15	20.0	73.580	148.43	0.045	0.04570

Table 2. *Cont.*

Group 4: Diameter approx. 25 mm					
Sample No.	**Diameter (mm)**	**Load (kN)**	**Yield Strength $\sigma_{0.2}$ (MPa)**	**Real Shrinkage (mm)**	**Shrinkage Obtained by Modeling (mm)**
16	25.1	107.910	169.46	0.040	0.03795
17	25.0	88.290	149.60	0.030	0.03229
18	25.2	98.100	192.68	0.025	0.02742
19	24.8	88.290	169.87	0.040	0.03229
20	25.1	78.480	152.15	0.020	0.02462
Group 5: Diameter approx. 30 mm					
21	29.8	147.150	169.33	0.030	0.03362
22	29.9	156.960	215.54	0.045	0.04527
23	29.8	166.770	189.25	0.040	0.03913
24	29.8	156.960	166.72	0.055	0.04527
25	30.0	98.100	147.05	0.035	0.03306

In most groups, the modeling predicts shrinkage quite accurately, especially for the groups with diameters around 16 mm and 20 mm, where the average relative error is 12.12% and 9.12%, respectively. The highest modeling accuracy is observed in the groups with diameters around 25 mm and 30 mm, where the average relative error is 3.20% and −2.55%, respectively. Group 1 shows a higher average relative error (15.21%). The main reason for this decrease in accuracy may be due to hidden defects in the material. Polymeric materials can have internal heterogeneity such as different densities or the presence of micropores and inclusions, which can significantly affect the mechanical properties and shrinkage behavior. Such inhomogeneities are difficult to detect without the use of specialized inspection techniques. Nevertheless, the simulation predicts shrinkage quite accurately and allows stress analysis over the entire cross-section of the specimen.

The results obtained formed the basis of the developed repair technology. This technology has been successfully tested at the energy enterprises in Ukraine. Taking into account the recommendations for deepening the polymer material into the body of the part to be restored, it is necessary to first make grooves 2.5–3 mm high on the surface of the foundation slabs, as shown in Figure 11. Such values of recesses were adopted based on the recommendations obtained in the course of this study. The height of the exceeding layer is 1.0–1.5 mm.

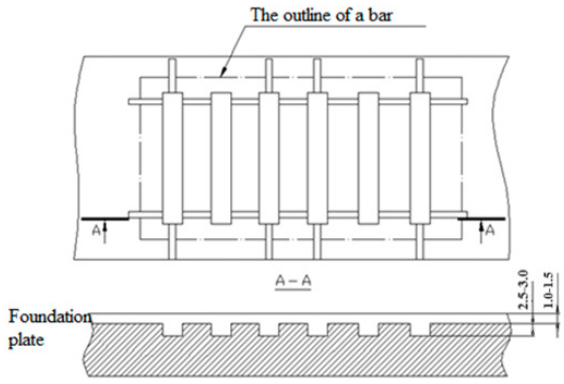

Figure 11. Sketch of the placement of pockets for multimetal 1018 on the surface of the foundation plate under the supporting surface of the bar. The pockets are connected by grooves for flowing and extruding multimetal 1018.

At the same time, to ensure adhesion, as well as accuracy when performing work, it is necessary to take into account the features of applying the composite multimetal 1018:

1. Clean the surfaces of the cylinder bonks and foundation plates and scrape until the non-flatness of the supporting surfaces is eliminated by no more than 0.5 mm;
2. Prepare four beacons for each bonk from a lead rod Ø 8–10 mm in thickness equal to 3 mm;
3. Along the perimeter of the installation site of compensation slabs (CP) on the foundation plate, stepping back from the CP by 1–1.5 mm weld a rod (wire) from each of its edges with a diameter equal to the thickness of the CP (Figure 12);
4. The supporting surface of the bonk, which will stand on the foundation plate without CP, and the plane of the bonk adjacent to it at 15–30 mm must be covered 1.5–2 h before repair with three layers of separator;
5. Lower the low-pressure cylinder (LPC) onto the adjustment screws and leave in this position for 24 h at 20 °C.

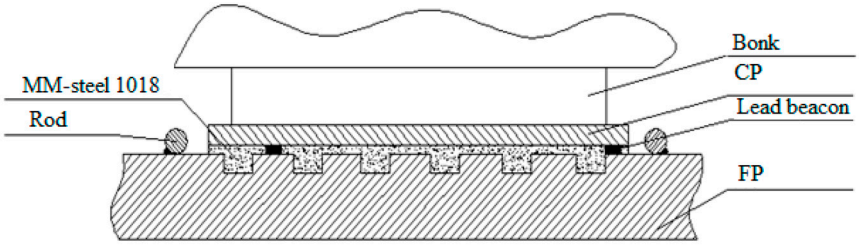

Figure 12. Scheme of installing a compensating plate on lead beacons in a space bounded by a welded rod (FP—fudament plate, CP—compensation plate).

Figure 12 shows a general view of the LPC housing with the cover removed, as well as the plane of the flange before and after applying the composite material (Figure 13).

Figure 13. General view of the LPC (low-pressure cylinder) housing with the cover removed.

The developed technology was successfully applied in the restoration of the surface of foundation plates during the installation of turbine generators TGV200 and LPC turbines K—200–180 LMZ of Starobeshevo thermal power plant and Zmievskaya thermal power plant. As a result of the final measurements of the gaps between the plane of the LPC bonks, set in the horizontal and vertical levels, and the plane of the plates, it was found that they were quite large. The use of the multimetal 1018 composite made it possible, firstly, to compensate for the resulting gaps and to obtain a snug fit of the bonks to the contact surface, as well as to protect the surface of the foundation slabs from further corrosive wear.

At the same time, under production conditions, it is not always possible to pre-make the grooves shown in Figure 5 on the supporting surface. Therefore, it is necessary to

restore the flatness of adjacent surfaces in a different way, limiting the flow of the composite material and at the same time, increasing its bearing capacity by enclosing it in a closed volume. Such a need arose during the repair of the LPC, in particular, when restoring its tightness along the line of contact between the cover and the body (Figure 13).

As can be seen from the Figure 14, the parting plane has an ideal surface formed by the mating surface of the flange of the LPC cover, which ensures the tightness of the internal cavity along the parting line. From a technical point of view, the photos shown here show a mating surface with pre-fused rollers. These rollers are used to limit the spread of the polymer material and also act as a support base for the mating surface.

(**a**) (**b**)

Figure 14. The plane of the flange (**a**) before and (**b**) after applying the composite material.

As shown by the 4-year operation of the turbine unit, there were no complaints about the tightness of the low-pressure pump.

4. Conclusions

1. Thus, it is obvious that with an increase in the contact area, the load-bearing capacity of the metal-polymer material multimetal 1018 increases with the same normal force acting on the samples.
2. As a result of loading the sample in various states, it was revealed that an additional support reduces deformation during compression, and also creates a reinforced structure that provides additional rigidity and resistance to impact. In addition, the closed volume ensured uniform load distribution throughout the entire volume of the sample. This prevented the formation of stress concentrations in certain areas and promoted more uniform compression.
3. Exceeding the material by 2.5 mm gives critical stress values for a closed sample at the level of 770 MPa, which, compared to the free version, corresponds to 205 MPa—an increase *in resistance by more than three times.*

Author Contributions: Conceptualization, A.I. and V.K.; methodology, A.I.; software, D.R. and R.B.; validation, A.A., O.N. and S.K.; formal analysis, D.R.; investigation, A.I., V.K. and D.R.; resources, A.I. and D.R.; data curation, A.I. and D.R.; writing—original draft preparation, A.I., D.R., D.S.; writing—review and editing, A.A., D.R.; visualization, D.R.; supervision, O.N.; project administration, A.I. and V.K.; funding acquisition, A.I. and D.S. All authors have read and agreed to the published version of the manuscript.

Funding: This research received no external funding.

Institutional Review Board Statement: Not applicable.

Data Availability Statement: The original contributions presented in the study are included in the article, further inquiries can be directed to the corresponding author/s.

Acknowledgments: We highly appreciate the support provided by HTWK Leipzig, as well as the assistance of Robert Böhm in obtaining the EFDS scholarship, which enabled the successful completion of this research.

Conflicts of Interest: The authors declare no conflicts of interest.

References

1. Bhuvaneswari, V. Chapter One—Recent advancements in polymer composites for damage repair applications. In *Polymer Composite Systems in Pipeline Repair*; Rangappa, S.M., Siengchin, S., Balaganesan, G., Kushvaha, V., Eds.; Gulf Professional Publishing: Oxford, UK, 2023; pp. 1–26.
2. Andrianov, I.V.; Danishevskyy, V.V.; Topol, H. Local stress distribution in composites for pulled-out fibers with axially varying bonding. *Acta Mech.* **2020**, *231*, 2065–2083. [CrossRef]
3. Wang, C.-M.; Ping, X.-C.; Wang, X.-X. Effects of local fiber discontinuity on the fatigue strength parameter at the fiber inclusion corner in fiber-reinforced composites. *Sci. Eng. Compos. Mater.* **2022**, *29*, 274–286. [CrossRef]
4. Ryzhov, N.I.; Durnev, A.I. Polymers and thermoplastic polyurethane elastomers in ship repair. *Shipbuild. Ship. Repair.* **2004**, *4*, 27–29.
5. Yang, M.; Akiyama, Y.; Sasaki, T. Evaluation of change in material properties due to plastic deformation. *J. Mater. Process. Technol.* **2004**, *151*, 232–236. [CrossRef]
6. Ischenko, A.; Rassokhin, D.; Nosovskaya, E. Restoration of rolled equipment using composite materials. *Report. Priazovskyi State Tech. Univ. Sect. Tech. Sci.* **2023**, *46*, 55–61.
7. Brown, E.N.; White, S.R.; Sottos, N.R. Retardation and repair of fatigue cracks in a microcapsule toughened epoxy composite—Part II: In situ self-healing. *Compos. Sci. Technol.* **2005**, *65*, 2474–2480. [CrossRef]
8. Cui, G.; Li, Z.L.; Yang, C. The influence of DC stray current on pipeline corrosion. *Pet. Sci.* **2016**, *13*, 135–145. [CrossRef]
9. Yang, W.; Ye, X.; Li, R.; Yang, J. Effect of Stray Current on Corrosion and Calcium Ion Corrosion of Concrete Reinforcement. *Materials* **2022**, *15*, 7287. [CrossRef] [PubMed]
10. Bertolini, L.; Carsana, M.; Pedeferri, P. Corrosion behaviour of steel in concrete in the presence of stray current. *Corros. Sci.* **2007**, *49*, 1056–1068. [CrossRef]
11. Leng, Z.; Wu, H.; Tang, X. Carbon nanotube/epoxy composites with low percolation threshold and negative dielectric constant. *J. Mater. Sci. Mater. Electron.* **2022**, *33*, 26015–26024. [CrossRef]
12. Bartoli, M.; Giorcelli, M.; Tagliaferro, A. Morphology and Mechanical Properties of Epoxy/Synthetic Fiber Composites. In *Handbook of Epoxy/Fiber Composites*; Mavinkere Rangappa, S., Parameswaranpillai, J., Siengchin, S., Thomas, S., Eds.; Springer: Singapore, 2022.
13. Piotr, S.; Kinga, P.; Stanislaw, B. Self-Healing Polyurethane-Based Nanocomposites Modified with Carbon Fibres and Carbon Nanotubes. *Adv. Polym. Technol.* **2020**, 1–13. [CrossRef]
14. Björkner, B. Plasticizers and Other Additives in Synthetic Polymers. In *Handbook of Occupational Dermatology*; Kanerva, L., Wahlberg, J.E., Elsner, P., Maibach, H.I., Eds.; Springer: Berlin/Heidelberg, Germany, 2000.
15. Wang, D.; Li, Y.; Xie, X.-M.; Guo, B.-H. Compatibilization and morphology development of immiscible ternary polymer blends. *Polymer* **2011**, *52*, 191–200. [CrossRef]
16. Hahladakis, J.N.; Velis, C.A.; Weber, R.; Iacovidou, E.; Purnell, P. An overview of chemical additives present in plastics: Migration, release, fate and environmental impact during their use, disposal and recycling. *J. Hazard. Mater.* **2018**, *344*, 179–199. [CrossRef] [PubMed]
17. Carradò, A.; Ravindra, N.M. Metal/Polymer/Metal Sandwich Systems: An Overview. *JOM* **2023**, *75*, 5126–5140. [CrossRef]
18. Paladugu, S.R.M.; Sreekanth, P.S.R.; Sahu, S.K.; Naresh, K.; Karthick, S.A.; Venkateshwaran, N.; Ramoni, M.; Mensah, R.A.; Das, O.; Shanmugam, R. A Comprehensive Review of Self-Healing Polymer, Metal, and Ceramic Matrix Composites and Their Modeling Aspects for Aerospace Applications. *Materials* **2022**, *15*, 8521. [CrossRef] [PubMed]
19. Kessler, M.R.; Sottos, N.R.; White, S.R. Self-healing structural composite materials. *Compos. A Appl. Sci. Manuf.* **2003**, *34*, 743–753. [CrossRef]
20. Yoshida, F.; Uemori, T.; Fujiwara, K. Elastic–plastic behavior of steel sheets under in-plane cyclic tension–compression at large strain. *Int. J. Plast.* **2002**, *18*, 633–659. [CrossRef]
21. Alexander, A.; Tzeng, J. Three Dimensional Effective Properties of Composite Materials for Finite Element Applications. *J. Compos. Mater.* **1997**, *31*, 466–485. [CrossRef]
22. Michel, J.; Moulinec, H.; Suquet, P. Effective properties of composite materials with periodic microstructure: A computational approach. *Comput. Methods Appl. Mech. Eng.* **1999**, *172*, 109–143. [CrossRef]
23. Özkir, S.E. Effect of restoration material on stress distribution on partial crowns: A 3D finite element analysis. *J. Dent. Sci.* **2018**, *13*, 311–317. [CrossRef]
24. Salam, S.S.; Mehat, N.M.; Kamaruddin, S. Optimization of Laminated Composites Characteristics via integration of Chamis Equation, Taguchi method and Principal Component Analysis. In Proceedings of the IOP Conference Series: Materials Science and Engineering, Bangkok, Thailand, 4–5 February 2019; Volume 551.

25. Bukowska, M.; Kasza, P.; Moska, R.; Jureczka, J. The Young's Modulus and Poisson's Ratio of Hard Coals in Laboratory Tests. *Energies* **2022**, *15*, 2477. [CrossRef]
26. Cózar, I.R.; Arbeláez-Toro, J.J.; Maimí, P.; Otero, F.; González, E.V.; Turon, A.; Camanho, P.P. A novel methodology to measure the transverse Poisson's ratio in the elastic and plastic regions for composite materials. *Compos. Part B Eng.* **2024**, *272*, 111098. [CrossRef]
27. Pham, D.C. Minimum energy and iteration estimates for longitudinal Young's modulus and Poisson's ratio of transversely-isotropic unidirectional composites. *Mech. Mater.* **2021**, *160*, 103983. [CrossRef]
28. Sun, H.; Di, S.; Zhang, N.; Wu, C. Micromechanics of composite materials using multivariable finite element method and homogenization theory. *Int. J. Solids Struct.* **2001**, *38*, 3007–3020. [CrossRef]
29. Manda, M.S.; Mat Rejab, M.R.; Hassan, S.A.; Wahit, M.U.; Nurhadiyanto, D. Experimental Study on Tin Slag Polymer Concrete Strengthening under Compression with Metallic Material Confinement. *Polymers* **2023**, *15*, 817. [CrossRef]
30. Forquin, P.; Nasraoui, M.; Rusinek, A.; Siad, L. Experimental study of the confined behaviour of PMMA under quasi-static and dynamic loadings. *Int. J. Impact Eng.* **2012**, *40–41*, 46–57. [CrossRef]